esurf-2018-72 (Lazarus *et al.*) – RESPONSE TO REVIEWERS

20 December 2018

Dear Editors –

Thank you for the opportunity to revise this submission. Following the constructive recommendations from our reviewers, we have made substantial changes to the manuscript, which we detail below.

We show reviewer comments in *italics*; our replies are in **bold**; and excerpts of new text are coloured blue.

Thank you for your continued time and consideration. We look forward to further correspondence.

Kind regards,

EDL (*et alia*)

Reviewer #1 (K Ratliff)

L26: perhaps caveat that the "large forcing events" that are shredded are relatively short-term, i.e., those operating on < months time scales

Amended sentence now reads (L26–27):

"This suggests that the physical effects of annual (or intra-annual) forcing events, including major storms, may convey less about the dynamics of long-term shoreline change…"

L131-133: The authors use the storm wave threshold (95th percentile of deep- water significant wave height) as a cutoff for the input flux time series. Particularly for the Argus dataset, it would be interesting and informative to compare the daily wave energy flux in its entirety to the shoreline change information (rather than just the storms). Are seasonal time scales evident in the daily wave energy flux time series? If so, this could be an interesting point of comparison (vs. the storm wave energy flux) that could strengthen the discussion of signal perseverance at longer time scales. An additional figure/histogram plotting the distribution of total wave energy for binned wave heights at Narrabeen-Collaroy beach from 2005- 2017 could also be useful to illustrate the relative influence of storm waves.

Much of the wave-forcing analysis that R#1 suggests has been published previously. To clarify and explain our use of storm waves (rather than a broader range of waves), we have revised this section to now read (L146–152):

"Previous work on Narrabeen-Collaroy has demonstrated that the relationship between wave-energy flux and shoreline change is strongest for storm waves (Harley et al., 2009; Phillips et al., 2017). By isolating storm waves, we do not mean to suggest that lower-energy waves do not move sediment. However, changes in nearshore bar and beach morphology tend to emerge far more slowly than the high-frequency variability of low-energy wave forcing (Plant et al., 2006), and, in this case, we are interested in the conditions under which an input flux could be preserved in the shoreline response signal. We defined storm wave conditions by a threshold corresponding to the 95th percentile of deep-water significant wave height…"

L138: include reference

We now cite Herbich (2000) (L159).

l. 226: "if climate-related drivers were to increase future forcing at the seasonal time-scale" – give an example of this – increasing storminess? Perhaps include a reference.

Now citing Emanuel (2013), we have amended this sentence to read (L283–286):

"Moreover, if climate-related drivers were to increase future forcing at the annual time-scale ($T \approx T_y$), perhaps through storm frequency or intensity or both (Emanuel, 2013), there is potential for system resonance (Binder et al., 1995; Cadot et al., 2003; Jerolmack and Paola, 2010) that could amplify corresponding shoreline changes."

L292-294: Re-word last sentence, as it does not read clearly.

Revised to now read (L332–334):

"In exploring the dynamics of signal shredding, controlled experiments would also illuminate characteristic time-scales for fundamental processes of sediment transport in coastal environments."

Figure 3B: Consider shortening x-axis to match 3A – I assume it's the same range as the Argus dataset, but the mismatch in x-scales between A and B and the data gap could be misleading and/or confusing.

In response to this and related comments, we have made an entirely new Fig. 2 – which absorbed the wave-related plots shown in the original Fig. 3. We have fixed offsets in plots of power spectra and scale ranges that previously complicated direct comparisons.

L172: correct spelling of "Ratliff" in reference (no 'e')

We have corrected the citation – with apologies for the typo.

l. 204: should reference figure 4B, not C

Corrected as noted (now in Fig. 3).

Reviewer #2

1. Explain why using the alongshore average of shoreline change is representative of the system (Fig. 2). It's unclear that it is the best metric to use for this spectral analysis, especially with rotational modes being the two primary contributors to shoreline change (Fig. 4).

Instead of using mean alongshore position to calculate shoreline change, we now present results based on the median absolute value of shoreline change at each position alongshore. Qualitatively, our results are the same (and perhaps even

cleaner). We also show the results of an alternative method, which takes the median of the underline power spectra from the absolute value of shoreline change at each position alongshore (in each of the three datasets). We present those ancillary results in a new pair of supplemental figures (Figs. S1 & S2), which also compare a wavelet-derived spectral analysis with a Fast Fourier Transform.

And, to explain how this treatment of the shoreline data dovetails with the embayed-beach dynamics discussed later in the manuscript (in Section 3.3), we have added the following (L258–268):

"Although resolved in two dimensions, these shoreline behaviours nevertheless inform our one-dimensional simplification of shoreline change (Fig. 2). The spatial analysis shows that at each position alongshore, shoreline position is moving onshore and offshore with a few dominant modes of sediment-transport dynamics that rework the embayed beach at characteristic time-scales. The "closed" system of the embayment makes the beach behave as a roughly conserved physical quantity. This means that rotation-driven shoreline change is spatially correlated, such that one side accretes approximately as much as the other side erodes. The spectral density of shoreline change over time at any position (y) is insensitive to this spatial correlation, because the absolute value of shoreline change makes the magnitudes at one end of the embayment approximately equal to those at the other, and thus their power spectra quantitatively similar, in turn."

2. What is the source of the data that was used to create figure 3? Should be added to "Setting and dataset" section. Is it from one source or multiple?

We now clarify that the wave data come from the Sydney waverider buoy:

"We also used deep-water wave data compiled from hourly records logged between 2005–2017 by the Sydney waverider buoy, located approximately 11 km offshore of the study area."

3. L143-148: Elaborate on the physical interpretation of the wave energy flux being unorganized and stationary in contrast to the transitional shoreline change. It seems there is a lack of intrinsic characteristic timescale, but why is that important to include?

We have significantly reworked this part of the manuscript (Section 3.1) to improve its clarity – not only by revising the text, but also by replacing the original Figs. 2 & 3 with a new Fig. 2.

The interpretation of the input signal now reads (L160–173):

"We calculated monthly and daily total storm-wave energy fluxes corresponding to the monthly and daily shoreline time-series (Fig. 2e,f), and transformed them into power spectra to demonstrate that the forcing (input) and response (output) spectra are not the same (Fig. 2d,g). Where the spectral density of shoreline change is non-stationary (correlated) over a range of relatively short time-scales (Fig. 2d), the spectral density of wave forcing is comparatively stationary (uncorrelated) over the same range (Fig. 2g). The monthly wave-energy time-series shows a peak in spectral density at ~24 mos, but with no clear comparator in the shoreline-change spectra. The daily wave-energy spectrum rises at the long-interval end of its range to a broad peak at ~30–45 mos (Fig.

2g), which overlaps with a local maximum in the shoreline-change spectra at ~37–42 mos (Fig. 2d).

Even in this one-dimensional representation, the sediment-transport processes of shoreline change have transformed an input signal into a quantitatively distinct output signal. To place these input/output spectral patterns in the context of physical processes that might explain them, we explored characteristic time-scales of key embayed-beach dynamics."

4. Consider using your wave data (heights and periods) to calculate the expected sedi- ment flux using a variation of the CERC formula. How would this Qs signal compare to the signal produced by +/- values of shoreline change? Since the modes are rotational, it may be informative to use if AST is the majority of sediment fluxes. The modes of shoreline change by Ratliff and Murray suggest that there should be a causative link.

We do not pursue a calculation of expected sediment flux in this revision because we no longer call the output signal a flux (L105–108):

"In our beach example, rather than considering sediment flux directly, we tracked the change in shoreline position, d_x (in m), between consecutive time steps at a given position alongshore (y)."

A comment by A Ashton (below) makes a related suggestion.

Furthermore, we have tried – such as at L258–268, excerpted above (see R#2's first comment) – to better explain how patterns in the one-dimensional and two-dimensional representations of shoreline behaviour are related.

5. L 204 – 213: The authors describe the first two modes as rotational and detail how much change each mode accounts for, but do not describe the types of modes the third and fourth are. Though they represent little change, it would be helpful to include the mode. The magnitudes from the PCA analysis would also be helpful to include.

We now include this information in the text (L251–255) and in Fig. 3c.

6. In regime 1 of the spectral power plots in Figure 2 (where the spectral power is a power law function of time scale), is the slope of the power law curve meaningful? Is it different between the data sets? There should be more details in the text of what is/can be quantified out of the power law to lead to the interpretation of morphodynamic turbulence.

Our new Fig. 2 shows the power spectra from all three shoreline-position datasets relative to each other. We now include a slope of the non-stationary (correlated) reach of the power spectra, along with the following interpretation (L128–136):

"Like the sedimentary systems described by Jerolmack and Paola (2010), the spectral density of the one-dimensional shoreline-change term $d_x(t)$ yields a pattern with two regimes (Fig. 2d). A non-stationary regime extends over shorter time-scales, such that spectral density versus time-scale are correlated by a power law. This relationship transitions at ~9–11 mos into a comparatively stationary (uncorrelated) regime over longer intervals. (A power function fitted to the three spectra, combined, for scales up to ~12 mos, returns a scaling exponent = 0.66, but the physical significance this slope value remains unclear.) This two-regime pattern in the power spectrum (Jerolmack and Paola,

2010) serves as an initial indication that signal shredding may be inherent in the dynamics of sandy beach systems."

7. In Figure 2, the arrows are not explained. I think they are showing that the data from one plot goes into making the next, but it appeared at first that they were pointing to something unexplained. Please clarify the purpose of the arrows. Please clarify the type of data used for each plot. It's difficult to discern as is. Could also be clearer by labeling the columns. And it is easy to miss the timescales. A separate plot for timescales would make the connection clearer.

Again, we have addressed these elements by constructing a completely new figure.

8. Line 247 has a typo – extra "and" in the sentence.

Fixed, as suggested.

Commenter #3 (A Ashton)

L22. L23 "detailed" is used twice in a row meaning different things. Or undefined things.

Amended second use of "detailed" so that L21–22 now read:

"…shorelines retain almost no detailed information about their own past positions. Here, we use a high-frequency, multi-decadal observational record of shoreline position…"

L109-111. Could use more discussion of how shoreline change is converted to flux and the physical motivation behind this. Particularly here where this is first discussed. Also having read through this seems to be the full methods explanation. Overall the MS could use more detailed methods. In this case, the connection between the wave flux and shoreline changes needs to be made more explicit. Right now just implied. This also needs to be separated into the cross-shore (alongshore averaged) and the alongshore-varying examples used later.

We have used this comment to motivate significant revisions throughout Sections 3.1 & 3.3. We have expanded our methodological explanations wherever they appear, and we have made a particular effort to better link the shoreline-change and wave-energy time-series that we treat as system output and input, respectively.

L141-2. Why using "q" for something that is not directly flux. Leading.

L147. Overall, I feel that the -> q analogy is somewhat circumspect. I wish the authors could explain/justify much better. It strike me that they are forcing their results a bit too much into the specific framework of the Jerolmack and Paola (2010) rather then just being inspired by this work. The latter makes more sense as there are functional differences between the systems.

As we note above, to R#2, we no longer refer to the shoreline-change signal as a flux (L105–108).

Moreover, we have revised the bulk of this submission according to the spirit of this comment – that we be inspired by Jerolmack & Paola (2010) rather be strict

adherents to its template. Even in the coauthors' independent readings of this revision, the shift in presentation has improved the manuscript fundamentally.

L158. Explicitly define the criteria for beach width. This probably does not affect the results, as L is just a scaling coefficient. Maybe better to scale with max − min? My concern is that on many developed/anthropogenically affected beaches, the beach width itself is set by things like development, how dune lines are locally determined, and the location of symbolic fencing.

Indeed, because we normalize L, the definition of beach width does not affect the results. (In a previous draft, we used a definition of $max − min$, but ultimately opted to describe the "full" beach width captured by the cross-shore profile.) However, for clarity, we have amended this line to read (L183–186):

"We assume that the system size L is equivalent to maximum cross-shore beach width, defined here as the cross-shore distance from a fixed landward reference point to mean sea-level (Harley and Turner, 2008; Harley et al., 2011b)."

L195. Could reference other, older works on PCA analyses of beach signals. Just an idea, I do not have specific examples on hand.

We now refer (L231–232) to Winant et al., 1975; Aubrey, 1979; Clarke and Eliot, 1982; Hsu et al., 1994; Dail et al., 2000; and Short and Trembanis (2004).

L213. Overall I feel that a constitutive connection is missing between the analyses of Fig 2 and Fig 4. Analysis one (Fig 2) is alongshore-averaged shoreline position. Analysis two (Fig 4) is about modes of change of shoreline position about the average (or at last most modes are, such as rotation, breathing, etc.). It would be helpful add more glue to put these concepts together together.

We have worked to address this disconnect – which R#2 also raises – throughout Section 3 of the text, and by presenting entirely new Figs. 2 & 4 (where the latter is a synthesis figure, as recommended below).

L232. I feel that overall the rice pile analogue is overemphasized. This example is constantly forced but the field site is not. I presume Fig 3 is meant to convey that there is weak spectral forcing in the data, but that should be different than constant forcing, no?

We have removed this discussion of the rice-pile analogue from the text (in keeping with the "inspired by" comment, above), and have clarified (with the new Fig. 2) our presentation and interpretation of input forcing.

L246-7. Um?

Revised, as suggested.

L250. Add some references here.

For the clause "… if most of the sediment shifted off a beach during a storm is stored in a nearshore bar and then swept back onshore in a matter of days to weeks afterward…" (L290–292), we now include Birkemeier (1979), List et al. (2006), and Phillips et al. (2017).

Fig 2. Please make this figure easier to read. The whole alphabet is not needed to signify the plots (not referenced as such in the text). Would be better to give titles to the columns and find a way to make the row descriptions more obvious (not hidden in the axis text).

Addressed, with an entirely new Fig. 2.

Fig 4. Please use color or at the very least different line types here.

Revised, as suggested (now Fig. 3).

Overall, I think that the MS could benefit from some form of summary plot/s. Values such as the tc for the different analyses should be summarized to make the point. Instead we are left with the spiderweb thin blue lines on the plots. On the log scale nobody can even read what these numbers are. I'm not a big fan of tables, but at the least a table of the T values would help. Even better if a plot could be figured out.

Addressed with an entirely new Fig. 2,and with the addition of a new Fig. 4 as a "synthesis" plot and a new Table 1 listing all of the characteristic time-scales across the various input/output time-series and analyses.

1 # Environmental signal shredding on sandy coastlines

2 Eli D. Lazarus[1]*, Mitchell D. Harley[2], Chris E. Blenkinsopp[3] and Ian L. Turner[2]

3 [1]Environmental Dynamics Lab, School of Geography and Environment, University of
4 Southampton, Southampton, UK

5 [2]Water Research Laboratory, School of Civil and Environmental Engineering, University of
6 New South Wales, Sydney NSW, Australia

7 [3]Research Unit for Water, Environment and Infrastructure Resilience (WEIR), University
8 of Bath, Bath, UK

9 *correspondence to: E.D.Lazarus@soton.ac.uk

10 **ORCIDs**

11 Lazarus   0000-0003-2404-9661
12 Harley   0000-0002-1329-7945
13 Blenkinsopp   0000-0001-5784-2805
14 Turner   0000-0001-9884-6917

15

16

17 **Abstract**

18 How storm events contribute to long-term shoreline change over decades to centuries
19 remains an open question in coastal research. Sand and gravel coasts exhibit remarkable
20 resilience to event-driven disturbances, and, in settings where sea level is rising, shorelines
21 retain almost no detailed information about their own past positions. Here, we use a high-
22 frequency, multi-decadal observational record of shoreline position to demonstrate
23 quantitative indications of morphodynamic turbulence – "signal shredding" – in a sandy
24 beach system. We find that, much as in other dynamic sedimentary systems, processes of
25 sediment transport that affect shoreline position at relatively short time-scales may obscure
26 or erase evidence of external forcing. This suggests that the physical effects of annual (or
27 intra-annual) forcing events, including major storms, may convey less about the dynamics
28 of long-term shoreline change – and vice versa – than coastal researchers might wish.

29

30 **Keywords –** coastal hazard; landscape resilience; beach recovery; beach rotation;
31 Narrabeen-Collaroy

1. Introduction

Quantifying magnitudes and rates of shoreline change is fundamental to understanding the dynamics of coastlines: not only how they behave over time, but also how they may respond to future changes in environmental forcing. From a coastal-management perspective, shoreline change may constitute a coastal hazard – either event-driven, like the impact of a major storm, or chronic, like persistent shoreline erosion from a net-negative sediment budget. Long-term, continuous measurement of shoreline position observed at a given location will record changes arising from event-driven and chronic forcing, alike. But how punctuated storm events contribute to long-term shoreline change over decades to centuries remains an open question, particularly in the context of shoreline-change prediction (Morton et al., 1994; Fenster et al., 2001; Houser and Hamilton, 2009; Anderson et al., 2010; Masselink and van Heteren, 2014; Brooks et al., 2016; Masselink et al., 2016; Scott et al., 2016; Burvingt et al., 2017).

Evidence of coastal storm frequency and magnitude over centuries to millennia may be stored in the sedimentary stratigraphy of beach ridges (Tamura, 2012) and washover into back-barrier lagoons (Donnelly and Woodruff, 2007). Ridge and washover stratigraphy offers a window into climatic forcing conditions in the recent geologic past, but is not a direct measure of shoreline position. Indeed, in transgressive settings (in which relative sea level is rising) the shoreline itself retains almost no detailed information about its own past positions. Sand and gravel coastlines, especially, reflect remarkable resilience to event-driven disturbances – even to tsunami (Choowong et al., 2009). Storm-driven shoreline excursions on the order of $\sim 10^1$–10^2 m may be obscured within days to months, and effectively erased within years (Birkemeir, 1979; Egense, 1989; Thom and Hall, 1991; Morton et al., 1994; Douglas and Crowell, 2000; Honeycutt et al., 2001; Zhang et al., 2002; List et al., 2006; Lazarus et al., 2012; Lentz et al., 2013; Coco et al., 2014; Masselink and van Heteren, 2014; Phillips et al., 2017).

This coastal context exemplifies a unifying challenge in geomorphology: determining how dynamic sedimentary systems – especially source-to-sink pathways – respond to rapid external forcing. Processes of sediment transport tend to rework upstream/upslope inputs so completely that their downstream/downslope outputs may bear no resemblance to the original pattern of forcing that drove them. In their essential synthesis of the problem, Jerolmack and Paola (2010) call this phenomenon the "shredding" of environmental signals. They offer that shredding – or, more formally, "morphodynamic turbulence" – behaves much like fluid turbulence, in that "energy injected at one frequency is smeared across a range of scales." High-frequency signals of external forcing are especially likely to be shredded. Drawing on the physics of turbulent fluid flows (Frisch and Kolmogorov, 1995), Jerolmack and Paola (2010) used time-series of sediment flux from physical and numerical experiments – bedload transport in a flume channel (Singh et al., 2009), a canonical rice-pile experiment (Frette et al., 1996), and a numerical rice-pile model – to illustrate their argument. Beyond source-to-sink sedimentary systems (Romans et al., 2016), signal shredding has since been extended to spatio-temporal changes in lake levels (Williams and Pelletier, 2015) and methane release from peatlands (Ramirez et al., 2015).

Here, we investigate signal shredding in an altogether different sediment-transport system: that of a sandy beach. Although previous studies of sandy shoreline dynamics have invoked signal shredding conceptually (Lazarus et al., 2011a, 2012; Williams et al., 2013), none have used observations of shoreline position to demonstrate quantitative signatures of signal shredding empirically. Following Jerolmack and Paola (2010), we find the hallmarks of morphodynamic turbulence in time-series of shoreline position measured at Narrabeen-Collaroy Beach, in southeast Australia (Short and Trembanis, 2004; Harley et al. 2011a, 2015; Turner et al. 2016; Phillips et al., 2017). The potential for beaches to "shred" large-magnitude changes in shoreline position forced at relatively short (~intra-annual) time-scales complicates reconciliation of short-term beach dynamics and long-term, spatio-temporal patterns of shoreline variability and evolution.

2. Setting and datasets

The Narrabeen-Collaroy embayment (Fig. 1a) holds a sandy beach 3.6 km long, and is one of only a few sites worldwide where ongoing beach monitoring has been regular, frequent, and uninterrupted for multiple decades (Turner et al., 2016). Cross-shore profiles at five locations along the beach (Fig. 1a) have been measured approximately monthly (Fig. 1b) since 1976 (Turner et al., 2016). In addition, continuous alongshore shoreline positions derived from RTK-GPS quad-bike surveys of the full three-dimensional subaerial beach have been recorded approximately monthly (Fig. 1c) between 2005–2017 (Harley and Turner 2008; Harley et al., 2011a, 2011b, 2015). Daily-averaged shoreline position in the southern half of the embayment (Fig. 1a) has also been captured by an Argus Coastal Imaging system (Fig. 1d) for over a decade (Phillips et al., 2017). In each of these datasets we used the 0.7 m AHD (Australian Height Datum) elevation contour to define the cross-shore shoreline position (x) at all positions alongshore (y), commensurate with mean high water (Harley et al., 2011a, 2011b). Data gaps in the profiles and time-series were filled by linear interpolation. We also used deep-water wave data compiled from hourly records logged between 2005–2017 by the Sydney waverider buoy, located approximately 11 km offshore of the study area.

3. Analysis

3.1. Patterns in power spectra

In their bedload and rice-pile examples, Jerolmack and Paola (2010) collapsed these physical systems into one dimension – a time-series of sediment flux past a single point. In our beach example, rather than considering sediment flux directly, we tracked the change in shoreline position, d_x (in m), between consecutive time steps at a given position alongshore (y). In a generic source-to-sink system in which sediment only moves downstream, sediment flux is unidirectional and positive. By contrast, in a one-dimensional treatment of a beach system, shoreline movement (d_x) is bidirectional, as wave-driven cross-shore sediment transport shifts the shoreline at any location onshore and offshore over time. To therefore include both onshore (negative) and offshore (positive) movement, we worked with the absolute value of shoreline change and calculated the power spectrum of the time-series using wavelet analysis, following the method described by Lazarus et al. (2011a,

2012). We show results based on the median absolute value of shoreline change for all positions alongshore at a given time step (Fig. 2a–c). To confirm that this simplification is representative, we also analysed the spectral density of the shoreline-change time-series at each position alongshore (Fig. S1).

This application of wavelet analysis functions much like a Fourier transform (Lazarus et al., 2011a, 2012). We first convolved the time-series (the absolute value of shoreline change) with a second-order Daubechies wavelet in a continuous wavelet transform. Taking the mean transform variance at temporal scales up to approximately half the overall length of the signal produced a measure of spectral power. We chose a wavelet with a small number of vanishing moments – a measure of how much the wavelet shape undulates – because simple wavelets tend to have better sensitivity over a greater range of scales. The general pattern of spectral density was insensitive to different wavelets with low vanishing moments, and was comparable to spectra generated by a Fast Fourier Transform (Fig. S2).

Like the sedimentary systems described by Jerolmack and Paola (2010), the spectral density of the one-dimensional shoreline-change term $d_x(t)$ yields a pattern with two regimes (Fig. 2d). A non-stationary regime extends over shorter time-scales, such that spectral density versus time-scale are correlated by a power law. This relationship transitions at ~9–11 mos into a comparatively stationary (uncorrelated) regime over longer intervals. (A power function fitted to the three spectra, combined, for scales up to ~12 mos, returns a scaling exponent = 0.66, but the physical significance this slope value remains unclear.) This two-regime pattern in the power spectrum (Jerolmack and Paola, 2010) serves as an initial indication that signal shredding may be inherent in the dynamics of sandy beach systems.

But what environmental signal is being shredded at the shoreline? Consider again a unidirectional source-to-sink system, driven by some input flux at the upstream end. That input flux might be constant; it might fluctuate quasi-periodically; it might spike with large-magnitude events. In a controlled physical experiment or a numerical model, input flux (of sediment and/or fluid) is a known quantity, set by the researcher. Whatever its pattern in time, input flux embodies the environmental signal that is susceptible to shredding by sediment-transport processes internal to the system. Here, for the beach system, we treated energy flux from incident storm waves as the external environmental signal that shoreline behaviour may destroy or preserve.

Previous work on Narrabeen–Collaroy has demonstrated that the relationship between wave-energy flux and shoreline change is strongest for storm waves (Harley et al., 2009; Phillips et al., 2017). By isolating storm waves, we do not mean to suggest that lower-energy waves do not move sediment. However, changes in nearshore bar and beach morphology tend to emerge far more slowly than the high-frequency variability of low-energy wave forcing (Plant et al., 2006), and, in this case, we are interested in the conditions under which an input flux could be preserved in the shoreline response signal. We defined storm wave conditions by a threshold corresponding to the 95th percentile of deep-water significant wave height (H_s, m), which for this region is $H_s > 3$ m (Harley, 2017). Much like

4

155   flow discharge in a fluvial system, deep-water wave energy flux (E, kW per m wavefront)
156   may serve as a useful proxy for input flux to the beach:

157    $$E = \frac{\rho g^2}{64\pi} H_s^2 P_w \approx 0.5 H_s^2 P_w \qquad\qquad\qquad (1)$$

158   where ρ (kg/m^3) is water density, g (m/s^2) is acceleration by gravity, H_s (m) is significant
159   deep-water wave height, and P_w (s) is wave period (Herbich, 2000).

160   We calculated monthly and daily total storm-wave energy fluxes corresponding to the
161   monthly and daily shoreline time-series (Fig. 2e,f), and transformed them into power
162   spectra to demonstrate that the forcing (input) and response (output) spectra are not the
163   same (Fig. 2d,g). Where the spectral density of shoreline change is non-stationary
164   (correlated) over a range of relatively short time-scales (Fig. 2d), the spectral density of
165   wave forcing is comparatively stationary (uncorrelated) over the same range (Fig. 2g). The
166   monthly wave-energy time-series shows a peak in spectral density at ~24 mos, but with no
167   clear comparator in the shoreline-change spectra. The daily wave-energy spectrum rises at
168   the long-interval end of its range to a broad peak at ~30–45 mos (Fig. 2g), which overlaps
169   with a local maximum in the shoreline-change spectra at ~37–42 mos (Fig. 2d).

170   Even in this one-dimensional representation, the sediment-transport processes of shoreline
171   change have transformed an input signal into a quantitatively distinct output signal. To
172   place these input/output spectral patterns in the context of physical processes that might
173   explain them, we explored characteristic time-scales of key embayed-beach dynamics.

174   **3.2 Characteristic time-scale from system size and input flux**

175   Jerolmack and Paola (2010) showed in their exemplars that the transition from non-
176   stationary to stationary (correlated to uncorrelated) in the spectral density of the output
177   signal occurs at an intrinsic, characteristic time-scale T_c. Theoretically, T_c is set by the
178   system size L relative to the constant (~mean) signal input. While those parameters can be
179   dictated for experimental systems, they are less clear for an open sandy coastline. To
180   independently estimate T_c in the Narrabeen-Collaroy system and compare the results to the
181   time-scale (or range of time-scales) at which the shoreline-change power spectra transition
182   from non-stationary to stationary, we tested two different approaches.

183   The first approach is a back-of-the-envelope exercise. We assumed that the system size L is
184   equivalent to maximum cross-shore beach width, defined here as the cross-shore distance
185   from a fixed landward reference point to mean sea level (Harley and Turner, 2008; Harley
186   et al., 2011b). This assumption extends from having collapsed the system into only the
187   cross-shore (x) dimension: at any alongshore position (y), the theoretical maximum cross-
188   shore (x) extent to which the beach can ever erode is the full width of the beach L,
189   independent of embayment length. (We call L the "theoretical maximum" because
190   historical records of shoreline change are necessarily of finite duration, and therefore may
191   never reflect this full width.) We normalised L relative to its maximum value, such that the
192   theoretical maximum $L = 1$. For the input flux, we took the mean normalised monthly
193   (and daily) total wave-energy flux over the full span of the dataset, which here serves the
194   purpose for a rough estimate of T_c. Using monthly total storm-wave energy flux (Fig. 2e),

L/E (where L and E are both normalised) yields T_c = 4–6 months; using the daily total storm-wave energy flux (Fig. 2f), T_c = 5–6 months. (These ranges come from excluding and including, respectively, zero values in the total wave-energy time-series, which increases or decreases the mean normalised E.) Note that this estimate aligns with a detailed analysis of time-scales for beach recovery at Narrabeen–Collaroy (Phillips et al., 2017). Plotted in relation to the power spectra for shoreline change (Fig. 2d), the characteristic time-scale marks approximately where the spectral density "rolls over" from non-stationary to stationary (correlated to uncorrelated), just ahead of the distinct local maximum at ~9–11 months.

3.3 Characteristic time-scale from modes of embayed beach dynamics

The second approach to estimate one or more characteristic time-scales T_c for the Narrabeen-Collaroy system derives from shoreline behaviours typical of this site, and of embayed beaches more generally (Short and Trembanis, 2004; Ranasinghe et al., 2004; Harley et al., 2011a, 2015; Ratliff and Murray, 2014).

Although they vary in detail between specific locations, approximately four modes of shoreline behaviour tend to describe how sediment moves within embayed beach systems. One mode represents sediment cycling offshore and onshore as a quasi-coherent unit at the full scale of the embayment: imagine a narrow beach during stormier times of the year, and a wide beach during calmer intervals. Another common mode is termed "rotation," and occurs when prevailing wave conditions or a storm event shifts a significant volume of sediment inside the embayment alongshore to form a wider beach at one end and a narrower beach at the other (Ranasinghe et al., 2004). Related to rotation is what has been described as a "breathing" mode, a kind of shoreline resonance that hinges near the centre of the beach and characterises changes in shoreline curvature, as sand moves between the middle and ends of an embayment (Ratliff and Murray, 2014). An additional mode of shoreline dynamics reflects patterns of shoreline variability introduced by rhythmic movements of sandbars, sandwaves, megacusps, and inlet processes, where applicable (Harley et al., 2011a, 2015). These four modes are not necessarily hierarchical: their relative dominance can change as a function of wave conditions (Harley et al., 2011a, 2015). More importantly, these modes of shoreline behaviour likely manifest intrinsic time-scales.

To find characteristic time-scales corresponding to the modes of shoreline behaviour at Narrabeen-Collaroy, we followed steps described by Ratliff and Murray (2014). From the monthly shorelines derived from RTK-GPS quad-bike surveys, at each position alongshore we detrended the series of shoreline position (not shoreline-position change) in time (Fig. 3a). To calculate the empirical orthogonal modes in the alongshore dimension through time, and thus characterise shoreline variation around its mean position (Fig. 3b), we applied principal-component analysis (Winant et al., 1975; Aubrey, 1979; Clarke and Eliot, 1982; Hsu et al., 1994; Dail et al., 2000; Short and Trembanis, 2004). Each mode in sequence explains a smaller percentage of variation in the data. We then used a continuous wavelet transform, again finding the mean transform variance over a range of time intervals (Lazarus et al., 2011a), to examine the spectral signatures of the first four behavioural

modes in the temporal dimension. In the resulting power spectrum, peaks represent the characteristic time-scale for each behavioural mode (Ratliff and Murray, 2014). We take T_c (Fig. 3c) as the first local maximum in the power spectrum (Ratliff and Murray, 2014), using a Ricker-Marr wavelet. (Other Gaussian-type wavelets yielded similar power spectra and characteristic time-scales.)

The first two modes in these data are both rotational (Fig. 3b). The first, a rotation toward the north, accounts for 51% of the observed shoreline variability with a peak time-scale at ~21 months (and a local saddle at ~12 months). The second, a rotation toward the south, accounts for 32% (~6–7 months) and agrees closely with the T_c calculated independently from the normalised storm wave-energy flux. In previous applications of PCA to >25 years of long-term profile data (Short and Trembanis, 2004) and 5 years of quad-bike measurements (Harley et al., 2011a, 2015) at Narrabeen-Collaroy, rotational behaviour was secondary (26% of shoreline variability around its mean position) to a dominant mode (~60%) of quasi-coherent, off- and onshore sand movement within the embayment. In the extended quad-bike dataset used here (Fig. 3a), bi-directional rotation appears to become the predominant mode after ~2010. The third and fourth modes account for 5.4% (~10–11 months) and 2.5% (~10–11 months) of observed shoreline variability, respectively, and might reflect "breathing" behaviour at the fulcrum and both ends of the beach, perhaps with influences from other sources of shoreline variability, including an ephemeral inlet near Narrabeen Headland (Fig. 1a). Approach angles of deep-water waves associated with different types of storm system likely control the occurrence and relative strengths of the various modes (Harley et al., 2011a, 2015).

Although resolved in two dimensions, these shoreline behaviours nevertheless inform our one-dimensional simplification of shoreline change (Fig. 2). The spatial analysis shows that at each position alongshore, shoreline position is moving onshore and offshore with a few dominant modes of sediment-transport dynamics that rework the embayed beach at characteristic time-scales. The "closed" system of the embayment makes the beach behave as a roughly conserved physical quantity. This means that rotation-driven shoreline change is spatially correlated, such that one side accretes approximately as much as the other side erodes. The spectral density of shoreline change over time at any position (y) is insensitive to this spatial correlation, because the absolute value of shoreline change makes the magnitudes at one end of the embayment approximately equal to those at the other, and thus their power spectra quantitatively similar, in turn.

4. Discussion and implications

Jerolmack and Paola (2010) showed that morphodynamic turbulence will tend to "shred" (strongly modify) input perturbations with time-scales shorter than the characteristic time-scale of the system ($T < T_c$). Only input perturbations with time-scales $T > T_c$ are likely to be preserved (or only weakly modified) in the output signal. The various characteristic time-scales that we estimated for the Narrabeen-Collaroy system (Fig. 4; Table 1) suggest that input perturbations (i.e., wave-energy events) with time-scales on the order of $T <$ ~10^1 months are subject to distortion by morphodynamic turbulence, and their effects on

shoreline change will tend to get "smeared" across a range of temporal scales in the output signal (Fig. 4).

By extension, irregular but multi-annual forcings, such as the El Niño–Southern Oscillation (ENSO), might have a time-scale sufficiently long enough to avoid erasure by annual cycling (Barnard et al., 2015). The power spectra for the shoreline-change and daily-resolution storm-wave energy flux register a peak near a time interval of ~3–4 years, consistent with ENSO forcing. Moreover, if climate-related drivers were to increase future forcing at the annual time-scale ($T \approx T_y$), perhaps through storm frequency or intensity or both (Emanuel, 2013), there is potential for system resonance (Binder et al., 1995; Cadot et al., 2003; Jerolmack and Paola, 2010) that could amplify corresponding shoreline changes.

However, the collective effect of these various and variable characteristic time-scales is to make storm-driven perturbations difficult to isolate in sparsely sampled records of shoreline change. If cross-shore beach recovery is rapid – that is, if most of the sediment shifted off a beach during a storm is stored in a nearshore bar and then swept back onshore in a matter of days to weeks afterward (Birkemeier, 1979; List et al., 2006; Phillips et al., 2017) – then the magnitude of shoreline change driven by a storm event may appear damped even in a monthly survey of beach position. When such large fluctuations are so ephemeral, only high-frequency sampling can hope to capture their fullest extents (Splinter et al., 2013; Phillips et al., 2017). And even then, nearshore beach dynamics may still ultimately obscure the magnitude of direct environmental forcing because of the complex transformation that offshore wave energy undergoes across the surf zone (Plant et al., 2006; Coco et al., 2014).

Intrinsic time-scales for behavioural modes of beach change along open coastlines may be different from those for embayed settings. Where alongshore spatial scales are large (~10^1–10^2 km), the cumulative, diffusive effect of alongshore sediment transport is an especially effective shredder (Lazarus et al., 2011a, 2012). Ratliff and Murray (2014) suggest the diffusive scaling evident in their modelling results implies that characteristic time-scales increase nonlinearly with embayment length alongshore. They list other factors that could likewise change the characteristic time-scales, such as wave height, sediment type, and the aspect ratio of headlands relative to the bay (which would affect local wave height through wave shadowing). Broadly posed, where the influence of alongshore sediment transport is significant and the beach system is "open" (rather than "closed" by headlands that make sand a conserved quantity), then the longer the beach, the more effective the system will be at shredding high-frequency signals. Were the same high-resolution spatio-temporal data available for ~10^4 m of open sandy coastline as it is for Narrabeen-Collaroy, a comparable analysis might highlight a series of progressively larger characteristic time-scales for reversing erosion hotspots, alongshore sand waves, and fluctuations in alongshore curvature (List et al., 2006; Lazarus and Murray, 2007, 2011; Lazarus et al., 2011a, 2012). Signal shredding may be strongest when coupled to human manipulations of natural shoreline behaviour (McNamara and Werner, 2008a, 2008b; Williams et al., 2013; Lazarus et al., 2011b; Lazarus et al., 2016).

In an ideal source-to-sink sedimentary system with perfect storage, output flux would be faithfully recorded in the sink stratigraphy. The majority of work in morphodynamic turbulence and signal shredding comes from efforts to puzzle out what information stratigraphic records do and do not convey about environmental forcing (Paola et al., 2018). For beach systems, that may mean large forcing events like major coastal storms, even when we can record their effects, probably tell us less about the dynamics of long-term shoreline change – and vice versa – than we would wish to know. Empirical evidence of signal shredding in the shoreline-position data from the Narrabeen-Collaroy system demonstrates how, and suggests why, signatures of individual storm impacts can be obscured or erased in long-term observational records, even those recorded at a reasonably high temporal resolution. Jerolmack and Paola (2010) recommend using controlled experiments to gain vital mechanistic insight into morphodynamic turbulence. Here, the effects of system size, input flux, the magnitudes of major disturbance events and potential resonant amplification ($T \approx T_s$) could be tested systematically across a broad parameter space for coastal systems. In exploring the dynamics of signal shredding, controlled experiments would also illuminate characteristic time-scales for fundamental processes of sediment transport in coastal environments.

Acknowledgements

350 **References**

351 Anderson, T. R., Frazer L. N., and Fletcher C. H.: Transient and persistent shoreline
352 change from a storm, Geophys. Res. Lett., 37, L08401, doi:10.1029/2009GL042252, 2010.

353 Ashton, A., Murray, A. B., and Arnault, O.: Formation of coastline features by large-scale
354 instabilities induced by high-angle waves, Nature, 414(6861), 296–300, 2001.

355 Ashton, A. D., and Murray, A. B.: High-angle wave instability and emergent shoreline
356 shapes: 1. Modeling of sand waves, flying spits, and capes, J. Geophys. Res. Earth, 111(F4),
357 doi:10.1029/2005JF000422, 2006a.

358 Ashton, A. D., and Murray, A. B.: High-angle wave instability and emergent shoreline
359 shapes: 2. Wave climate analysis and comparisons to nature, J. Geophys. Res. Earth,
360 111(F4), doi:10.1029/2005JF000423, 2006b.

361 Aubrey, D. G.: Seasonal patterns of onshore-offshore sediment movement, J. Geophys.
362 Res., 84(C10), 6347–6354, 1979.

363 Barnard, P. L., Short, A. D., Harley, M. D., Splinter, K. D., Vitousek, S., Turner, I. L.,
364 Allen, J., Banno, M., et al.: Coastal vulnerability across the Pacific dominated by El
365 Niño/Southern Oscillation, Nat. Geosci., 8(10), 801–807, 2015.

366 Binder, G., Tardu, S., and Vezin, P.: Cyclic modulation of Reynolds stresses and length
367 scales in pulsed turbulent channel flow, Proc. R. Soc. Lond. A, 451(1941), 121–139, 1995.

368 Birkemeier, W. A.: The effects of the 19 December 1977 coastal storm on beaches in
369 North Carolina and New Jersey, USACE Coastal Engineering Research Center, 1979.

370 Brooks, S. M., Spencer, T., McIvor, A., and Möller, I: Reconstructing and understanding
371 the impacts of storms and surges, southern North Sea, Earth Surf. Proc. Land., 41(6), 855–
372 864, 2016.

373 Burvingt, O., Masselink, G., Russell, P., and Scott, T.: Classification of beach response to
374 extreme storms, Geomorphology, 295, 722–737, 2017.

375 Cadot, O., Titon, J. H., and Bonn, D.: Experimental observation of resonances in
376 modulated turbulence, J. Fluid Mech., 485, 161–170, 2003.

377 Choowong, M., Phantuwongraj, S., Charoentitirat, T., Chutakositkanon, V., Yumuang, S.,
378 and Charusiri, P.: Beach recovery after 2004 Indian Ocean tsunami from Phang-nga,
379 Thailand, Geomorphology, 104(3), 134–142, 2009.

380 Clarke, D. J., and Eliot, I.: Description of littoral, alongshore sediment movement from
381 empirical eigen-function analysis, J. Geol. Soc. Aust., 29, 327–341, 1982.

382 Coco, G., Senechal, N., Rejas, A., Bryan, K. R., Capo, S., Parisot, J. P., Brown, J. A., and
383 MacMahan, J. H. M.: Beach response to a sequence of extreme storms, Geomorphology,
384 204, 493–501, 2014.

385 Dail, H. J., Merrifield, M. A., and Bevis, M.: Steep beach morphology changes due to
386 energetic wave forcing, Mar. Geol., 162(2–4), 443–458, doi:10.1016/S0025-3227(99)00072-
387 9, 2000.

388 Donnelly, J. P., and Woodruff, J. D.: Intense hurricane activity over the past 5,000 years
389 controlled by El Niño and the West African monsoon, Nature, 447(7143), 465–468, 2007.

390 Douglas, B. C., and Crowell, M.: Long-term shoreline position prediction and error
391 propagation, J. Coastal Res., 16(1), 145–152, 2000.

Egense, A. K.: Southern California beach changes in response to extraordinary storm, Shore and Beach, 57(4), 14–17, 1989.

Emanuel, K. A.: Downscaling CMIP5 climate models shows increased tropical cyclone activity over the 21st century, Proc. Nat. Acad. Sci. USA, 110(30), 12219–12224, 2013.

Fenster, M. S., Dolan, R., and Morton, R. A.: Coastal storms and shoreline change: signal or noise? J. Coastal Res., 17(3), 714–720, 2001.

Frette, V., Christensen, K., Malthe-Sorenssen, A., and Feder, J.: Avalanche dynamics in a pile of rice, Nature, 379(6560), 49–52, 1996.

Frisch, U., and Kolmogorov, A. N.: Turbulence: The legacy of A.N. Kolmogorov, Cambridge Univ. Press, Cambridge, 1995.

Harley, M. D.: Coastal storm definition, in: Ciavola, P., Coco, G. (Eds.), Coastal Storms: Processes and Impacts, John Wiley and Sons, 1–21, 2017.

Harley, M. D., and Turner, I. L.: A simple data transformation technique for pre-processing survey data at embayed beaches, Coastal Eng., 55(1), 63–68, 2008.

Harley, M. D., Turner, I. L., Short, A. D., and Ranasinghe, R.: An empirical model of beach response to storms – SE Australia, in: Coasts and Ports 2009: In a Dynamic Environment (Engineers Australia), Wellington, New Zealand, 600–606, 2009.

Harley, M. D., Turner, I. L., Short, A. D., and Ranasinghe, R.: A reevaluation of coastal embayment rotation: The dominance of cross-shore versus alongshore sediment transport processes, Collaroy-Narrabeen Beach, southeast Australia, J. Geophys. Res. Earth, 116(F4), doi:10.1029/2011JF001989, 2011a.

Harley, M. D., Turner, I. L., Short, A. D., and Ranasinghe, R.: Assessment and integration of conventional, RTK-GPS and image-derived beach survey methods for daily to decadal coastal monitoring. Coastal Eng., 58(2), 194–205, 2011b.

Harley, M. D., Turner, I. L., and Short, A. D.: New insights into embayed beach rotation: The importance of wave exposure and cross-shore processes, J. Geophys. Res. Earth, 120(8), 1470–1484, 2015.

Herbich, J. B.: Handbook of Coastal Engineering, McGraw-Hill, New York, 2000.

Honeycutt, M. G., Crowell, M., and Douglas, B. C.: Shoreline-position forecasting: impact of storms, rate-calculation methodologies, and temporal scales, J. Coastal Res., 17(3), 721–730, 2001.

Hsu, T. W., Ou, S. H., and Wang, S. K.: On the prediction of beach changes by a new 2-D empirical eigenfunction model, Coastal Eng., 23(3–4), doi: 10.1016/0378-3839(94)90005-1, 255–270, 1994.

Jerolmack, D. J., and Paola, C.: (2010). Shredding of environmental signals by sediment transport, Geophys. Res. Lett., 37(19), doi:10.1029/2010GL044638, 2010.

Lazarus, E. D., and Murray, A. B.: Process signatures in regional patterns of shoreline change on annual to decadal time scales, Geophys. Res. Lett., 34(19), doi:10.1029/2007GL031047, 2007.

Lazarus, E. D., and Murray, A. B.: An integrated hypothesis for regional patterns of shoreline change along the Northern North Carolina Outer Banks, USA. Mar. Geo., 281(1-4), 85–90, 2011.

Lazarus, E., Ashton, A., Murray, A. B., Tebbens, S., and Burroughs, S.: Cumulative versus transient shoreline change: Dependencies on temporal and spatial scale, J. Geophys. Res. Earth, 116(F2), doi:10.1029/2010JF001835, 2011a.

Lazarus, E. D., McNamara, D. E., Smith, M. D., Gopalakrishnan, S., and Murray, A. B.: Emergent behavior in a coupled economic and coastline model for beach nourishment, Nonlinear Proc. Geoph., 18, 989–999, 2011b.

Lazarus, E. D., Ashton, A. D., and Murray, A. B.: Large-scale patterns in hurricane-driven shoreline change, in Extreme events and natural hazards: the complexity perspective, Sharma, A. S., Bunde, A., Dimri, V. P. and Baker, D. N. (Eds.), AGU Geophysical Monograph Series, 196, 127–138, 2012.

Lazarus, E. D., Ellis, M. A., Murray, A. B., and Hall, D. M.: An evolving research agenda for human–coastal systems, Geomorphology, 256, 81–90, 2016.

Lentz, E. E., Hapke, C. J., Stockdon, H. F., and Hehre, R. E.: Improving understanding of near-term barrier island evolution through multi-decadal assessment of morphologic change, Mar. Geol., 337, 125–139, 2013.

List, J. H., Farris, A. S., and Sullivan, C.: (2006). Reversing storm hotspots on sandy beaches: spatial and temporal characteristics, Mar. Geol., 226, 261–279, 2006.

Masselink, G., and van Heteren, S.: Response of wave-dominated and mixed-energy barriers to storms. Mar. Geol., 352, 321–347, 2014.

Masselink, G., Castelle, B., Scott, T., Dodet, G., Suanez, S., Jackson, D., and Floc'h, F.: Extreme wave activity during 2013/2014 winter and morphological impacts along the Atlantic coast of Europe, Geophys. Res. Lett., 43(5), 2135–2143.

McNamara, D. E., and Werner, B. T.: Coupled barrier island–resort model: 1. Emergent instabilities induced by strong human-landscape interactions, J. Geophys. Res. Earth, 113(F1), doi:10.1029/2007JF000840, 2008a.

McNamara, D. E., and Werner, B. T.: Coupled barrier island–resort model: 2. Tests and predictions along Ocean City and Assateague Island National Seashore, Maryland, J. Geophys. Res. Earth, 113(F1), doi:10.1029/2007JF000841, 2008b.

Morton, R. A., Paine, J. G., and Gibeaut, J. C.: Stages and durations of post-storm beach recovery, southeastern Texas coast, USA, J. Coastal Res., 10(4), 884–908, 1994.

Paola, C., Ganti, V., Mohrig, D., Runkel, A. C., and Straub, K. M.: Time not our time: Physical controls on the preservation and measurement of geologic time, Annu. Rev. Earth Pl. Sci., 46, 409–438, 2018.

Phillips, M. S., Harley, M. D., Turner, I. L., Splinter, K. D., and Cox, R. J.: Shoreline recovery on wave-dominated sandy coastlines: the role of sandbar morphodynamics and nearshore wave parameters, Mar. Geol., 385, 146–159, 2017.

Plant, N. G., Holland, K. T., and Holman, R. A.: A dynamical attractor governs beach response to storms, Geophys. Res. Lett., 33(17), 2006.

Ramirez, J. A., Baird, A. J., Coulthard, T. J., and Waddington, J. M.: Ebullition of methane from peatlands: Does peat act as a signal shredder? Geophys. Res. Lett., 42(9), 3371–3379, 2015.

Ranasinghe, R., McLoughlin, R., Short, A., and Symonds, G.: The Southern Oscillation Index, wave climate, and beach rotation, Mar. Geol., 204(3-4), 273–287, 2004.

477 Ratliff, K. M., and Murray, A. B.: Modes and emergent time scales of embayed beach
478 dynamics, Geophys. Res. Lett., 41(20), 7270–7275, 2014.

479 Romans, B. W., Castelltort, S., Covault, J. A., Fildani, A., and Walsh, J. P.: Environmental
480 signal propagation in sedimentary systems across timescales, Earth-Sci. Rev., 153, 7–29,
481 2016.

482 Scott, T., Masselink, G., O'Hare, T., Saulter, A., Poate, T., Russell, P., Davidson, M. and
483 Conley, D.: The extreme 2013/2014 winter storms: Beach recovery along the southwest
484 coast of England, Mar. Geol., 382, 224–241, 2016.

485 Short, A. D., and Trembanis, A. C.: Decadal scale patterns in beach oscillation and rotation
486 Narrabeen Beach, Australia: time series, PCA and wavelet analysis, J. Coastal Res., 523–
487 532, 2004.

488 Singh, A., Fienberg, K., Jerolmack, D. J., Marr, J., and Foufoula-Georgiou, E.:
489 Experimental evidence for statistical scaling and intermittency in sediment transport rates,
490 J. Geophys. Res. Earth, 114(F1), doi:10.1029/2007JF000963, 2009.

491 Splinter, K. D., Turner, I. L., and Davidson, M. A.: How much data is enough? The
492 importance of morphological sampling interval and duration for calibration of empirical
493 shoreline models, Coastal Eng., 77, 14–27, 2013.

494 Tamura, T.: Beach ridges and prograded beach deposits as palaeoenvironment records,
495 Earth-Sci. Rev., 114(3-4), 279–297, 2012.

496 Thom, B. G., and Hall, W.: Behaviour of beach profiles during accretion and erosion
497 dominated periods, Earth Surf. Proc. Land., 16(2), 113–127, 1991.

498 Turner, I. L., Harley, M. D., Short, A. D., Simmons, J. A., Bracs, M. A., Phillips, M. S., and
499 Splinter, K. D.: A multi-decade dataset of monthly beach profile surveys and inshore wave
500 forcing at Narrabeen, Australia, Scientific Data, 3, doi:10.1038/sdata.2016.24, 2016.

501 Williams, Z. C., and Pelletier, J. D.: Self-affinity and surface-area-dependent fluctuations of
502 lake-level time series, Water Resour. Res., 51(9), 7258–7269, 2015.

503 Williams, Z. C., McNamara, D. E., Smith, M. D., Murray, A. B., and Gopalakrishnan, S.:
504 Coupled economic-coastline modeling with suckers and free riders, J. Geophys. Res. Earth,
505 118(2), 887–899, 2013.

506 Winant, C. D., Inman, D. L., and Nordstrom, C. E.: Description of seasonal beach changes
507 using empirical eigenfunctions, J. Geophys. Res., 80(15), 1979–1986, 1975.

508 Zhang, K., Douglas, B., and Leatherman, S.: Do storms cause long-term beach erosion
509 along the US East Barrier Coast? J. Geol., 110(4), 493–502, 2002.

Figures, Tables, and Captions

511

512
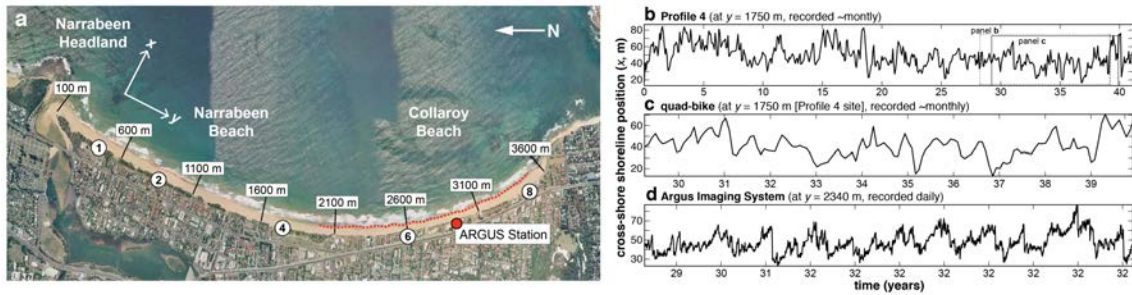
Figure 1. (a) Narrabeen-Collaroy beach, with locations of long time-series profiles and Argus Imaging System coverage. Alongshore coordinates (y) are relative to the northern end, below Narrabeen Headland. **(b)** Long-term time-series of cross-shore shoreline position (0.7 m contour) at Profile 4, measured approximately monthly between 1976–2017. Time axis is in years since first measurement (27 April 1976). **(c)** Time-series of cross-shore shoreline position at alongshore location y = 1750 m (aligned with Profile 4), measured by quad bike approximately monthly between 2005–2017. **(d)** Time-series of cross-shore shoreline position at alongshore location y = 2340 m, measured daily by an Argus Imaging System between 2005–2016. Boxes (dotted, solid) in panel (b) frame the temporal coverages for the time-series in panels (c) and (d).

523

**shoreline-change analysis (output signal)**

storm-wave analysis (input signal)
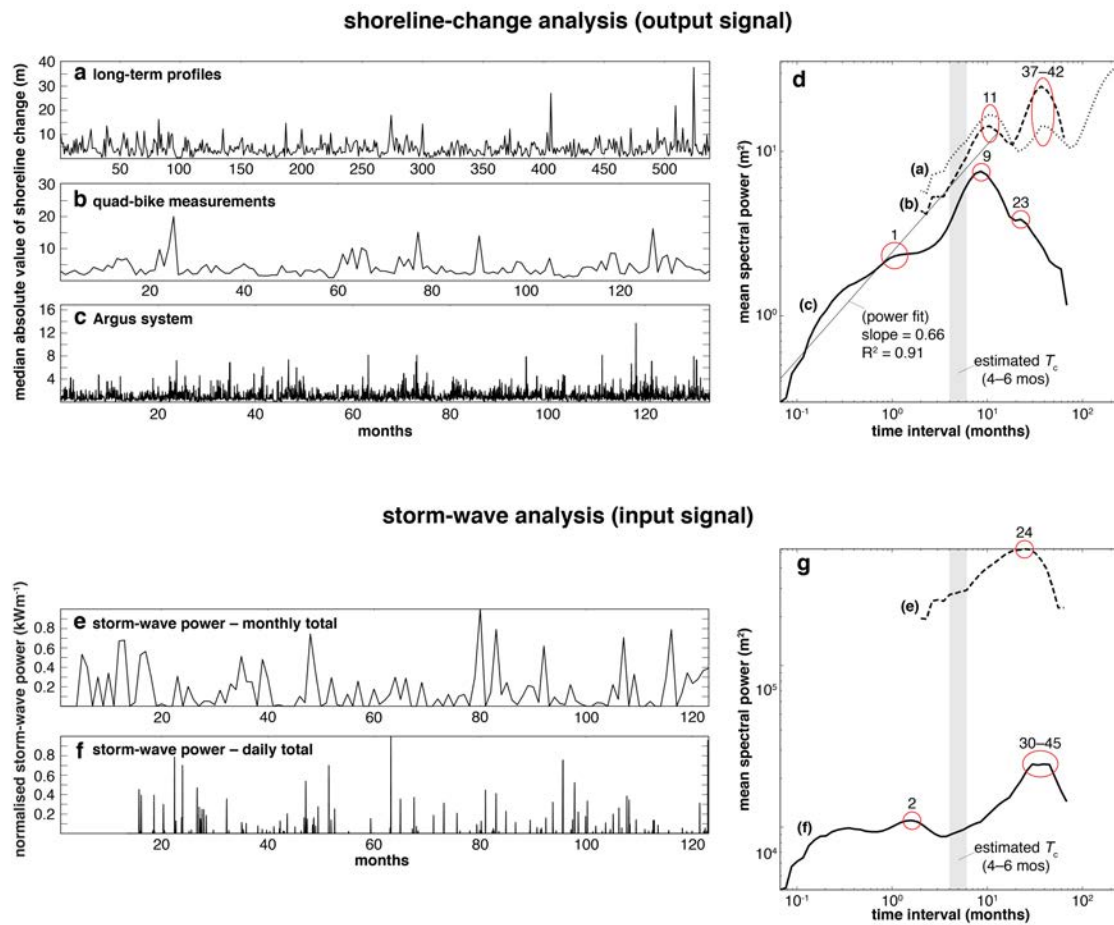
Figure 2. *Shoreline-change analysis (upper panels):* Alongshore median of the absolute value of monthly shoreline change from **(a)** long-term Profiles 1, 2, 4, 6, and 8, **(b)** monthly shoreline position from the RTK-GPS quad-bike surveys, and **(c)** a 850 m reach of the Argus coverage (y = 1950–2800 m). **(d)** Wavelet-derived power spectra for the three shoreline-change signals, respectively, showing a transition from non-stationary to stationary at time-scales ~10^1 mos. A power function fitted to the three spectra, combined, for scales up to ~12 mos, returns a scaling exponent = 0.66. *Storm-wave analysis (lower panels):* **(e)** Monthly and **(f)** daily total storm wave-energy flux between 2005–2017 (normalised to their respective maxima), used here to represent forcing input. **(g)** Power spectra for the storm-wave energy flux in (e) and (f). Labelled circles emphasise major peaks in spectral density at various time scales. Grey bar in (d) and (g) indicates an estimated characteristic time-scale T_c = 4–6 months, based on normalised beach width relative to mean normalised wave-energy forcing.

540

541
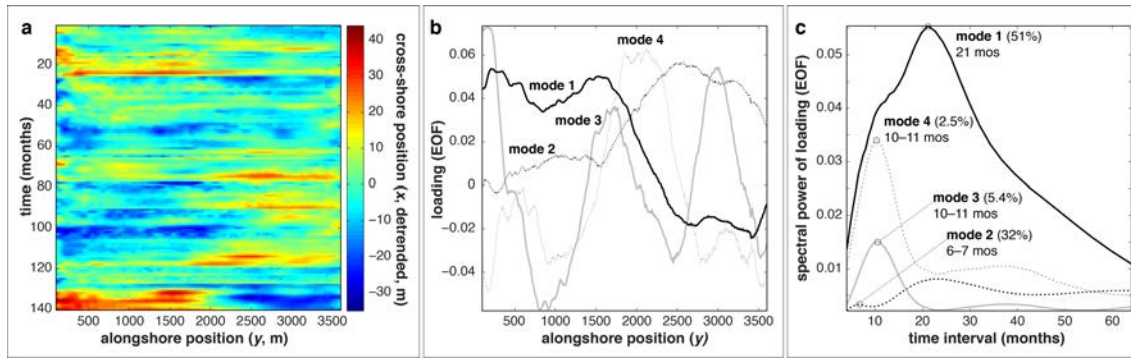
Figure 3. (a) Detrended (in time) shoreline position, measured approximately monthly by quad bike, with north at left (corresponding to Fig. 1a). **(b)** Orthogonal PCA modes, representing variance about the mean shoreline position, and **(c)** wavelet-derived power spectra of each mode, where the first local maximum indicates the characteristic time-scale for that mode.

547

548
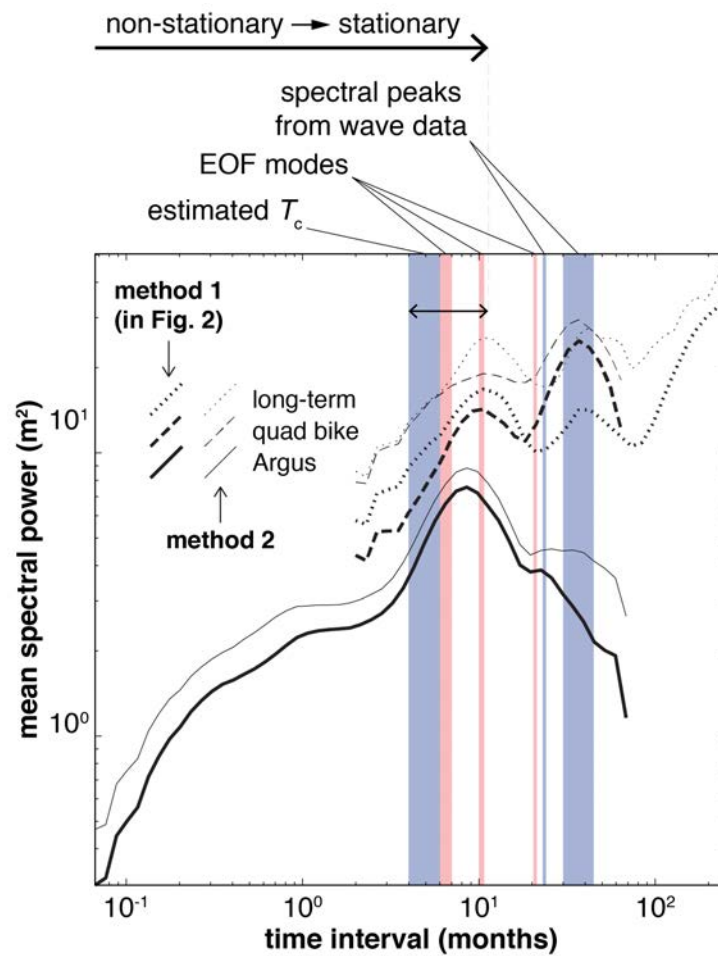
549

550 **Figure 4.** Compilation of power spectra from shoreline-change data in relation to different
551 characteristic time-scales for environmental forcing (blue/dark bars) and intrinsic physical
552 processes (red/light bars). Thick black lines indicate power spectra shown in Fig. 2d,
553 derived from the alongshore median absolute value of shoreline change through time
554 ("method 1"). Thin grey lines show the median spectral densities of power spectra of
555 shoreline change through time (detrended, absolute value) at each position alongshore for
556 the three survey types ("method 2"), shown in Fig. S1. We plot them together here to
557 demonstrate their comparability. Double-ended arrow indicates transition zone in the
558 spectral density from non-stationary to stationary by a temporal interval on the order of
559 $\sim 10^1$ months.

560

561 **Table 1.** Compilation of characteristic time-scales in Figs. 2 & 4.

Data source	Characteristic time-scales (mos)
Shoreline-change datasets	
Method 1 (alongshore median absolute value of shoreline change)	
long-term profiles (monthly)	11, 37–42
quad-bike surveys (monthly)	11, 37–42
Argus system (daily)	~1, 9, 23
Method 2 (median spectral power of absolute value of shoreline change over time at each position alongshore)	
long-term profiles (monthly)	11–12, 42, 56
quad-bike surveys (monthly)	12, 37–42
Argus system (daily)	~1, 8–10, 26, 34
Storm-wave energy forcing	
estimated T_c (normalised L/E)	4–6
storm-wave E flux (monthly)	24
storm-wave E flux (daily)	~2, 30–45
EOF modes of embayed beach behaviour	
Mode 1 (51%, rotational)	12–14, 21
Mode 2 (32%, rotational)	6–7, 22–26
Mode 3 (5.4%, breathing & other)	10–11, 36–42
Mode 4 (2.5%, breathing & other)	10–11, 36–42

562